Roman NIESTRÓJ, Tadeusz BIAŁOŃ, Marian PASKO

Silesian University of Technology, Institute of Electrical Engineering and Informatics

Stability analysis of the MRAS-type estimator taking into account parameter changes of the model of the induction motor

Abstract. *The paper presents the results of stability and reconstruction quality analysis performed for MRAS-type estimator in steady-state of rotor speed and stator and rotor magnetic fluxes of induction motor, obtained with taking into consideration simultaneous changes of all parameters of induction motor model. Investigations were performed for a large number of sets of motor's model parameters with random deviations. Investigation results were worked out statistically.*

Streszczenie. *W niniejszym artykule przedstawiono wyniki badania stabilności i jakości odtwarzania w estymatorze MRAS w stanie ustalonym prędkości wirnika i strumieni magnetycznych stojana i wirnika silnika indukcyjnego, uzyskane przy uwzględnieniu jednoczesnych zmian wszystkich parametrów modelu silnika indukcyjnego. Badania wykonano dla dużej liczby zbiorów parametrów modelu silnika z losowymi odchyłkami. Wyniki badania zostały opracowane statystycznie. (**Analiza stabilności estymatora MRAS z uwzględnieniem zmienności parametrów modelu silnika indukcyjnego**).*

Keywords: induction motor, MRAS-type estimator, stability analysis, state variables reconstruction.
Słowa kluczowe: silnik indukcyjny, estymator MRAS, analiza stabilności, odtwarzanie zmiennych stanu.

Introduction

MRAS-type estimators (Model Reference Adaptive System), used in the induction motor control systems for angular rotor speed ω_r and magnetic fluxes of the stator $\underline{\psi}_s$ and rotor $\underline{\psi}_r$ reconstruction, belong to a class of adaptive direct systems (for which adaptation mechanism influences directly some parameter of the adaptive system, in this case ω_r) [1]. Block diagram of a classical MRAS-type estimator is shown in the figure 1. Principle of operation and properties of different versions of this estimator (with different quantities used as signals $\boldsymbol{w}_{\mathrm{ref}}$ and $\boldsymbol{w}_{\mathrm{adapt}}$) are described in the publications [2,3] as well as in the publications cited there.

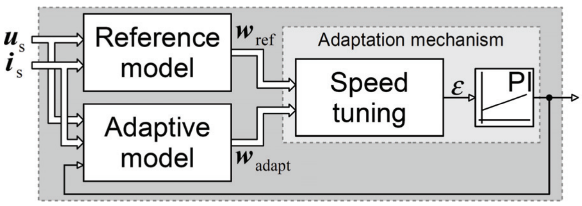

Fig. 1. Block diagram of a classical MRAS-type estimator

In this paper MRAS-type estimator with induction motor acting as reference model is presented, for different types of adaptive model. This solution is free from disadvantages related to low quality of reference model, specific for the classical structure of the MRAS-type estimator. The quality of the presented MRAS-type estimator depends on the quality of the applied adaptive model. Presented MRAS-type estimator is provided with the proportional-integral adaptation mechanism, consisting of the generator of a speed tuning signal ε and the proportional-integral regulator acting as an adaptive unit. In the presented estimator signal ε is expressed as electromagnetic torque [4].

For investigation of MRAS-type estimators' stability the second Lyapunov's principle is usually applied [4]. However, it is difficult to use, bearing in mind deviations of motor model parameters. Investigation of reconstruction quality of MRAS-type estimators is usually performed taking into consideration changes of only one of the motor's model parameters [3,5]. Taking into consideration the fact that MRAS-type estimator is a non-linear system, this method is inconvenient.

Equations of the MRAS-type estimator

The induction motor, as a mono-harmonic machine with one rotor circuit and linear magnetic circuit, can be described with use of following state and output equations (in Cartesian coordinate system, rotating with any speed ω_x):

(1) $$\dot{\boldsymbol{x}} = \left(\boldsymbol{A}_{\mathrm{m}}(\omega_{\mathrm{x}}) + \omega_{\mathrm{r}}\boldsymbol{L}_{\mathrm{m}}\right)\boldsymbol{x} + \boldsymbol{B}_{\mathrm{m}}\boldsymbol{u}_{\mathrm{s}},$$

(2) $$\boldsymbol{i}_{\mathrm{s}} = \boldsymbol{C}_1\boldsymbol{x},\ \ \boldsymbol{\psi}_{\mathrm{r}} = \boldsymbol{C}_2\boldsymbol{x},\ \ \boldsymbol{\psi}_{\mathrm{s}} = \boldsymbol{C}_{3\mathrm{m}}\boldsymbol{x},$$

where: ω_r – electrical angular speed of the rotor, symbol • denotes the first time derivative.

Vectors: state variables $\boldsymbol{x}$, inputs $\boldsymbol{u}_s$ and outputs: $\boldsymbol{i}_s$, $\boldsymbol{\Psi}_r$ and $\boldsymbol{\Psi}_s$ are described with following equations:

(3) $$\boldsymbol{x} = \left[i_{\mathrm{sx}}\ \ i_{\mathrm{sy}}\ \ \psi_{\mathrm{rx}}\ \ \psi_{\mathrm{ry}}\right]^{\mathrm{T}},\ \ \boldsymbol{u}_{\mathrm{s}} = \left[u_{\mathrm{sx}}\ \ u_{\mathrm{sy}}\right]^{\mathrm{T}},$$
$$\boldsymbol{i}_{\mathrm{s}} = \left[i_{\mathrm{sx}}\ \ i_{\mathrm{sy}}\right]^{\mathrm{T}},\ \ \boldsymbol{\psi}_{\mathrm{r}} = \left[\psi_{\mathrm{rx}}\ \ \psi_{\mathrm{ry}}\right]^{\mathrm{T}},\ \ \boldsymbol{\psi}_{\mathrm{s}} = \left[\psi_{\mathrm{sx}}\ \ \psi_{\mathrm{sy}}\right]^{\mathrm{T}}.$$

State, input and output matrices, occurring in the equations (1) and (2), have following forms:

(4)
$$\boldsymbol{A}_{\mathrm{m}}(\omega_{\mathrm{x}}) = \begin{bmatrix} a_{11\mathrm{m}}(\omega_{\mathrm{x}}) & a_{12\mathrm{m}} \\ a_{21\mathrm{m}} & a_{22\mathrm{m}}(\omega_{\mathrm{x}}) \end{bmatrix},$$
$$a_{11\mathrm{m}}(\omega_{\mathrm{x}}) = \left(R_{\mathrm{rm}}\frac{a_{\mathrm{m}}^2}{c_{\mathrm{m}}} + R_{\mathrm{sm}}c_{\mathrm{m}}\right)\boldsymbol{I} - \omega_{\mathrm{x}}\boldsymbol{J},$$
$$a_{12\mathrm{m}} = R_{\mathrm{rm}}a_{\mathrm{m}}\left(b_{\mathrm{m}} - \frac{a_{\mathrm{m}}^2}{c_{\mathrm{m}}}\right)\boldsymbol{I},\ \ a_{21\mathrm{m}} = R_{\mathrm{rm}}\frac{a_{\mathrm{m}}}{c_{\mathrm{m}}}\boldsymbol{I},$$
$$a_{22\mathrm{m}}(\omega_{\mathrm{x}}) = R_{\mathrm{rm}}\left(b_{\mathrm{m}} - \frac{a_{\mathrm{m}}^2}{c_{\mathrm{m}}}\right)\boldsymbol{I} - \omega_{\mathrm{x}}\boldsymbol{J},$$
$$\boldsymbol{L}_{\mathrm{m}} = \begin{bmatrix} \boldsymbol{Z} & a_{\mathrm{m}}\boldsymbol{J} \\ \boldsymbol{Z} & \boldsymbol{J} \end{bmatrix},\ \ \boldsymbol{B}_{\mathrm{m}} = \begin{bmatrix} -c_{\mathrm{m}}\boldsymbol{I} \\ \boldsymbol{Z} \end{bmatrix},$$
$$\boldsymbol{C}_1 = \begin{bmatrix}\boldsymbol{I} & \boldsymbol{Z}\end{bmatrix},\ \ \boldsymbol{C}_2 = \begin{bmatrix}\boldsymbol{Z} & \boldsymbol{I}\end{bmatrix},\ \ \boldsymbol{C}_{3\mathrm{m}} = \begin{bmatrix} -\frac{1}{c_{\mathrm{m}}}\boldsymbol{I} & \frac{a_{\mathrm{m}}}{c_{\mathrm{m}}}\boldsymbol{I} \end{bmatrix},$$
$$\boldsymbol{I} = \begin{bmatrix} 1 & 0 \\ 0 & 1 \end{bmatrix},\ \ \boldsymbol{J} = \begin{bmatrix} 0 & -1 \\ 1 & 0 \end{bmatrix},\ \ \boldsymbol{Z} = \begin{bmatrix} 0 & 0 \\ 0 & 0 \end{bmatrix},$$
$$a_{\mathrm{m}} = \frac{L_{\mathrm{mm}}}{L_{\mathrm{mm}}^2 - L_{\mathrm{sm}}L_{\mathrm{rm}}},\ \ b_{\mathrm{m}} = \frac{L_{\mathrm{sm}}}{L_{\mathrm{mm}}^2 - L_{\mathrm{sm}}L_{\mathrm{rm}}},$$
$$c_{\mathrm{m}} = \frac{L_{\mathrm{rm}}}{L_{\mathrm{mm}}^2 - L_{\mathrm{sm}}L_{\mathrm{rm}}},$$
$$L_{\mathrm{sm}} = L_{\mathrm{s\sigma m}} + L_{\mathrm{mm}},\ \ L_{\mathrm{rm}} = L_{\mathrm{r\sigma m}} + L_{\mathrm{mm}},$$

where: R_{sm}, R_{rm}, $L_{\mathrm{s\sigma m}}$, $L_{\mathrm{r\sigma m}}$, L_{mm} – parameters of induction motor's equivalent scheme.

Presented model of an induction motor is a bilinear dynamic system. For reconstruction of state variables $\boldsymbol{x}$ and speed ω_{r} of the motor described with equations (1) and (2), a MRAS-type estimator can be applied, described with following generalized equations:

- for an adaptive model:

$$\dot{\hat{\boldsymbol{x}}} = \left[\boldsymbol{A}(\omega_{\mathrm{x}}) + \hat{\omega}_{\mathrm{r}}\boldsymbol{L} + (\boldsymbol{K}_1 + \hat{\omega}_{\mathrm{r}}\boldsymbol{K}_2)\boldsymbol{C}_1\right]\hat{\boldsymbol{x}} + \ldots \\ \ldots + \boldsymbol{B}_1\boldsymbol{u}_{\mathrm{s}} + \left(\boldsymbol{B}_2(\omega_{\mathrm{x}}) - \hat{\omega}_{\mathrm{r}}\boldsymbol{K}_2\right)\boldsymbol{i}_{\mathrm{s}} + \boldsymbol{B}_3\dot{\boldsymbol{i}}_{\mathrm{s}}, \tag{5}$$

- for a speed tuning signal:

$$\varepsilon = \left(i_{\mathrm{sx}} - \hat{i}_{\mathrm{sx}}\right)\hat{\psi}_{\mathrm{ry}} - \left(i_{\mathrm{sy}} - \hat{i}_{\mathrm{sy}}\right)\hat{\psi}_{\mathrm{rx}} = \ldots \\ \ldots = \left(\boldsymbol{i}_{\mathrm{s}}^{\mathrm{T}} - \hat{\boldsymbol{x}}^{\mathrm{T}}\boldsymbol{C}_1^{\mathrm{T}}\right)\boldsymbol{H}\hat{\boldsymbol{x}}, \quad \boldsymbol{H} = \left[\boldsymbol{Z} \quad -\boldsymbol{J}\right], \tag{6}$$

- for a proportional-integral adaptive unit:

$$\hat{\omega}_{\mathrm{r}} = K_{\mathrm{P}}\varepsilon + \frac{1}{T_{\mathrm{I}}}\int_0^{\tau}\varepsilon \,\mathrm{d}t, \tag{7}$$

- for input signals:

$$\hat{\boldsymbol{i}}_{\mathrm{s}} = \boldsymbol{C}_1\hat{\boldsymbol{x}}, \quad \hat{\boldsymbol{\psi}}_{\mathrm{r}} = \boldsymbol{C}_2\hat{\boldsymbol{x}}, \quad \hat{\boldsymbol{\psi}}_{\mathrm{s}} = \boldsymbol{C}_3\hat{\boldsymbol{x}}, \\ \boldsymbol{C}_3 = \left[-\frac{1}{c}\boldsymbol{I} \quad \frac{a}{c}\boldsymbol{I}\right], \tag{8}$$

where symbol ˆ denotes a quantity reconstructed in the MRAS-type estimator.

Block diagram of the MRAS-type estimator, described with equations (5) – (8), is presented in the figure 2. Block diagram of a generalized adaptive model, described with equation (5), is shown in the figure 3.

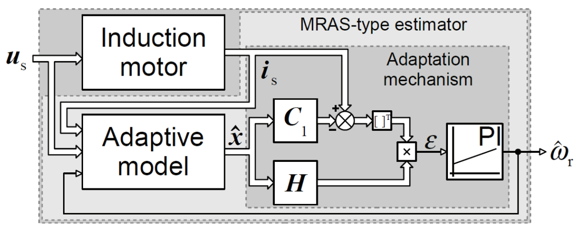

Fig. 2. Block diagram of the MRAS-type estimator

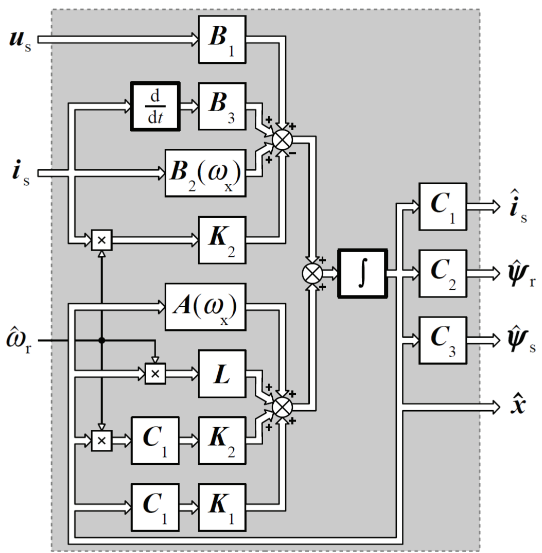

Fig. 3. Block diagram of the generalized adaptive model

Presented estimator is a non-linear dynamic system due to the form of equations (5) and (6). Matrix $\boldsymbol{A}(\omega_{\mathrm{x}})$, occurring in the equation (5), has a following form:

$$\boldsymbol{A}(\omega_{\mathrm{x}}) = \begin{bmatrix} a_{11}(\omega_{\mathrm{x}}) & a_{12} \\ a_{21} & a_{22}(\omega_{\mathrm{x}}) \end{bmatrix}, \\ a_{11}(\omega_{\mathrm{x}}) = \left(R_{\mathrm{r}}\frac{a^2}{c} + R_{\mathrm{s}}c\right)\boldsymbol{I} - \omega_{\mathrm{x}}\boldsymbol{J}, \\ a_{12} = R_{\mathrm{r}}a\left(b - \frac{a^2}{c}\right)\boldsymbol{I}. \tag{9}$$

Forms of the elements a_{21} and $a_{22}(\omega_{\mathrm{x}})$ of matrix $\boldsymbol{A}(\omega_{\mathrm{x}})$ and forms of other matrices, occurring in the equation (5), depend on particular form of applied adaptive unit. Following forms are possible:

- form 1 - voltage $\underline{\psi}_{\mathrm{r}}$ estimator operating together with $\underline{i}_{\mathrm{s}}$ estimator [2,6];

$$a_{21} = \boldsymbol{Z}, \quad a_{22}(\omega_{\mathrm{x}}) = -\omega_{\mathrm{x}}\boldsymbol{J}, \\ \boldsymbol{L} = \begin{bmatrix} \boldsymbol{Z} & a\boldsymbol{J} \\ \boldsymbol{Z} & \boldsymbol{Z} \end{bmatrix}, \quad \boldsymbol{B}_1 = \begin{bmatrix} -c\boldsymbol{I} \\ \frac{c}{a}\boldsymbol{I} \end{bmatrix}, \\ \boldsymbol{B}_2(\omega_{\mathrm{x}}) = \begin{bmatrix} \boldsymbol{Z} \\ -R_{\mathrm{s}}\frac{c}{a}\boldsymbol{I} + \omega_{\mathrm{x}}\frac{1}{a}\boldsymbol{J} \end{bmatrix}, \\ \boldsymbol{B}_3 = \begin{bmatrix} \boldsymbol{Z} \\ \frac{1}{a}\boldsymbol{I} \end{bmatrix}, \quad \boldsymbol{K}_1 = \boldsymbol{K}_2 = \begin{bmatrix} \boldsymbol{Z} \\ \boldsymbol{Z} \end{bmatrix}, \tag{10}$$

- form 2 - current $\underline{\psi}_{\mathrm{r}}$ estimator operating together with $\underline{i}_{\mathrm{s}}$ estimator [2,5];

$$a_{21} = \boldsymbol{Z}, \quad a_{22}(\omega_{\mathrm{x}}) = R_{\mathrm{r}}\left(b - \frac{a^2}{c}\right)\boldsymbol{I} - \omega_{\mathrm{x}}\frac{c}{a}\boldsymbol{J}, \\ \boldsymbol{L} = \begin{bmatrix} \boldsymbol{Z} & a\boldsymbol{J} \\ \boldsymbol{Z} & \boldsymbol{J} \end{bmatrix}, \quad \boldsymbol{B}_1 = \begin{bmatrix} -c\boldsymbol{I} \\ \boldsymbol{Z} \end{bmatrix}, \\ \boldsymbol{B}_2(\omega_{\mathrm{x}}) = \begin{bmatrix} \boldsymbol{Z} \\ R_{\mathrm{r}}\frac{a}{c}\boldsymbol{I} \end{bmatrix}, \quad \boldsymbol{B}_3 = \boldsymbol{K}_1 = \boldsymbol{K}_2 = \begin{bmatrix} \boldsymbol{Z} \\ \boldsymbol{Z} \end{bmatrix}, \tag{11}$$

- form 3 - Luenberger proportional observer [2,4];

$$a_{21} = R_{\mathrm{r}}\frac{a}{c}\boldsymbol{I}, \quad a_{22}(\omega_{\mathrm{x}}) = R_{\mathrm{r}}\left(b - \frac{a^2}{c}\right)\boldsymbol{I} - \omega_{\mathrm{x}}\boldsymbol{J}, \\ \boldsymbol{L} = \begin{bmatrix} \boldsymbol{Z} & a\boldsymbol{J} \\ \boldsymbol{Z} & \boldsymbol{J} \end{bmatrix}, \quad \boldsymbol{B}_1 = \begin{bmatrix} -c\boldsymbol{I} \\ \boldsymbol{Z} \end{bmatrix}, \quad \boldsymbol{B}_2 = -\boldsymbol{K}_1, \\ \boldsymbol{B}_3 = \begin{bmatrix} \boldsymbol{Z} \\ \boldsymbol{Z} \end{bmatrix}, \quad \boldsymbol{K}_1 = \begin{bmatrix} k_{111}\boldsymbol{I} \\ k_{131}\boldsymbol{I} \end{bmatrix}, \quad \boldsymbol{K}_2 = \begin{bmatrix} -k_{212}\boldsymbol{J} \\ -k_{232}\boldsymbol{J} \end{bmatrix}. \tag{12}$$

Non-zero elements of matrices $\boldsymbol{K}_1$ and $\boldsymbol{K}_2$ can be obtained with optimization method with use of genetic algorithm [7] or with poles (eigenvalues) of the observer location method so that they are proportional to the poles of the motor model, with factor of proportionality k [8]. In this second case, these elements are described with following equations:

$$k_{111} = (k-1)(R_{\mathrm{s}}c + R_{\mathrm{r}}b), \quad k_{212} = 1 - k, \\ k_{131} = \frac{1}{a}(1-k)(R_{\mathrm{s}}ck - R_{\mathrm{r}}b), \quad k_{232} = \frac{1}{a}(1-k). \tag{13}$$

- form 4 - state space simulator [9]. For this form equations (12) are valid, with the difference, that all elements of matrices $\boldsymbol{K}_1$ and $\boldsymbol{K}_2$ are equal to zero.

MRAS-type estimator stability analysis

The stability of linear dynamic system is tested with use of poles locus analysis of its transfer function [10]. For asymptotically stable system, all of poles λ_i of its transfer function are placed in the left part of complex plane ($\Re(\lambda_i) < 0$). MRAS-type estimator is a non-linear dynamic system, which is why the analysis of its stability with methods suitable for linear system can be performed after linearisation of its equations. Linearisation consists of obtaining linear equations describing non-linear dynamic system in the neighbourhood of steady operating point, where time derivatives of state variables are equal to zero [10]. For MRAS-type estimator the natural Cartesian coordinate system used for equation formation is the fixed system (ω_x=0) α–β. However, in this coordinate system, even in a steady state, state variables' transients are sine-like waveforms, therefore their time derivative is not equal to zero (this is so called quasi-steady state). The only coordinate system, in which proper linearisation of MRAS-type estimator is possible, is the system rotating with synchronous speed (ω_x=ω_s) d–q, in which following relationships are met:

$$\dot{\boldsymbol{x}}_0^{\mathrm{d-q}} = 0,\ \ \dot{\hat{\boldsymbol{x}}}_0^{\mathrm{d-q}} = 0,\ \ \dot{\boldsymbol{i}}_{\mathrm{s0}}^{\mathrm{d-q}} = 0, \tag{14}$$

where: superscript „d–q” denotes a quantity in d–q coordinate system, superscript „0” denotes value of the quantity in a steady operating point, in the neighbourhood of which the linearisation was performed.

Moreover, in a steady state of the MRAS-type estimator, the following equation is true (regardless of coordinate system adopted):

$$\varepsilon_0 = 0. \tag{15}$$

Transformation of MRAS-type estimator's equations into d–q coordinate system for the forms 1, 2, and 4 is easy and intuitive (it is sufficient to replace ω_x with ω_s in matrices $\boldsymbol{A}(\omega_x)$ and $\boldsymbol{B}_2(\omega_x)$). For form 3 it is possible to prove, that such an easy transformation is possible only when matrices $\boldsymbol{K}_1$ and $\boldsymbol{K}_2$ have appropriate forms (this matrices have to show some symmetry of elements).

Linearised equations of the MRAS-type estimator

Linearised equations of the MRAS-type estimator presented in Cartesian d–q coordinate system, rotating with synchronous speed ω_s, in the domain of the Laplace operator s, for increments Δ of quantities occurring in equations (5) – (8), may be expressed as:

- for adaptive model:

$$\begin{aligned}\Delta\hat{\boldsymbol{x}}^{\mathrm{d-q}} = (\boldsymbol{S}_4 - \boldsymbol{F}_0)^{-1}\Big[&\boldsymbol{B}_1\Delta\boldsymbol{u}_{\mathrm{s}}^{\mathrm{d-q}} + \ldots \\ &\ldots + (\boldsymbol{E}_{30} + \boldsymbol{B}_3\boldsymbol{S}_2)\Delta\boldsymbol{i}_{\mathrm{s}}^{\mathrm{d-q}} + \boldsymbol{E}_{40}\Delta\hat{\omega}_{\mathrm{r}}\Big],\end{aligned} \tag{16}$$

- for speed tuning signal:

$$\Delta\varepsilon = \boldsymbol{E}_{10}\Delta\hat{\boldsymbol{x}}^{\mathrm{d-q}} + \boldsymbol{E}_{20}\Delta\boldsymbol{i}_{\mathrm{s}}^{\mathrm{d-q}}, \tag{17}$$

- for proportional-integral adaptive unit:

$$\Delta\hat{\omega}_{\mathrm{r}} = K_{\mathrm{PI}}\Delta\varepsilon,\ \ K_{\mathrm{PI}} = K_{\mathrm{P}} + s^{-1}T_{\mathrm{I}}, \tag{18}$$

- for output signals:

$$\begin{aligned}\hat{\boldsymbol{i}}_{\mathrm{s}}^{\mathrm{d-q}} &= \hat{\boldsymbol{i}}_{\mathrm{s0}}^{\mathrm{d-q}} + \boldsymbol{C}_1\Delta\hat{\boldsymbol{x}}^{\mathrm{d-q}}, \\ \hat{\boldsymbol{\psi}}_{\mathrm{r}}^{\mathrm{d-q}} &= \hat{\boldsymbol{\psi}}_{\mathrm{r0}}^{\mathrm{d-q}} + \boldsymbol{C}_2\Delta\hat{\boldsymbol{x}}^{\mathrm{d-q}}, \\ \hat{\boldsymbol{\psi}}_{\mathrm{s}}^{\mathrm{d-q}} &= \hat{\boldsymbol{\psi}}_{\mathrm{s0}}^{\mathrm{d-q}} + \boldsymbol{C}_3\Delta\hat{\boldsymbol{x}}^{\mathrm{d-q}}.\end{aligned} \tag{19}$$

Matrices occurring in equations (16) and (17) may be expressed as:

$$\begin{aligned}&\boldsymbol{S}_4 = s\boldsymbol{I}_4,\ \ \boldsymbol{I}_4 = \begin{bmatrix}\boldsymbol{I} & \boldsymbol{Z}\\ \boldsymbol{Z} & \boldsymbol{I}\end{bmatrix},\ \ \boldsymbol{S}_2 = s\boldsymbol{I}, \\ &\boldsymbol{F}_0 = \boldsymbol{A}(\omega_{\mathrm{s}}) + \hat{\omega}_{\mathrm{r0}}\boldsymbol{L} + (\boldsymbol{K}_1 + \hat{\omega}_{\mathrm{r0}}\boldsymbol{K}_2)\boldsymbol{C}_1, \\ &\boldsymbol{E}_{10} = \left(\boldsymbol{i}_{\mathrm{s0}}^{\mathrm{d-q}}\right)^{\mathrm{T}}\boldsymbol{H} - \left(\hat{\boldsymbol{x}}_0^{\mathrm{d-q}}\right)^{\mathrm{T}}\left(\boldsymbol{C}_1^{\mathrm{T}}\boldsymbol{H} + \boldsymbol{H}^{\mathrm{T}}\boldsymbol{C}_1\right), \\ &\boldsymbol{E}_{20} = \left(\hat{\boldsymbol{x}}_0^{\mathrm{d-q}}\right)^{\mathrm{T}}\boldsymbol{H}^{\mathrm{T}}, \\ &\boldsymbol{E}_{30} = \boldsymbol{B}_2(\omega_{\mathrm{s}}) - \hat{\omega}_{\mathrm{r0}}\boldsymbol{K}_2, \\ &\boldsymbol{E}_{40} = (\boldsymbol{L} + \boldsymbol{K}_2\boldsymbol{C}_1)\hat{\boldsymbol{x}}_0^{\mathrm{d-q}} - \boldsymbol{K}_2\boldsymbol{i}_{\mathrm{s0}}^{\mathrm{d-q}}.\end{aligned} \tag{20}$$

Steady-state equations of the MRAS-type estimator

Due to deviations of parameters of the motor's equivalent scheme, the following relationships are true:

$$\begin{aligned}&R_{\mathrm{s}} \neq R_{\mathrm{sm}},\ \ R_{\mathrm{r}} \neq R_{\mathrm{rm}}, \\ &L_{\mathrm{s}\sigma} \neq L_{\mathrm{s}\sigma\mathrm{m}},\ \ L_{\mathrm{r}\sigma} \neq L_{\mathrm{r}\sigma\mathrm{m}},\ \ L_{\mathrm{m}} \neq L_{\mathrm{mm}}.\end{aligned} \tag{21}$$

These deviations are the cause of lasting reconstruction errors of magnetic fluxes $\underline{\psi}_s$, $\underline{\psi}_r$ and speed ω_r in MRAS-type estimator. Therefore, in general case, following dependence is true:

$$\delta w_0 \neq 0,\ \ \delta w_0 = \frac{\hat{w}_0 - w_0}{w_0}, \tag{22}$$

where: δw_0 is a relative reconstruction error of quantity w_0 in the steady operating point, w_0 is one of following quantities: ω_{r0}, $|\underline{\psi}_{s0}|$, $|\underline{\psi}_{r0}|$. The module of a rotor or stator magnetic flux $\underline{\psi}_0$ is calculated with following dependence:

$$\left|\underline{\psi}_0\right| = \sqrt{\left(\hat{\boldsymbol{\psi}}_0^{\mathrm{d-q}}\right)^{\mathrm{T}}\hat{\boldsymbol{\psi}}_0^{\mathrm{d-q}}}. \tag{23}$$

Value $\boldsymbol{i}_{\mathrm{s0}}^{\mathrm{d-q}}$ required in the equations (20) can be obtained by assuming values $\boldsymbol{u}_{\mathrm{s0}}^{\mathrm{d-q}}$, ω_s and ω_{r0}, taking into account equation (14) and solving for $\boldsymbol{x}_0^{\mathrm{d-q}}$ a following linear equation:

$$(\boldsymbol{A}_{\mathrm{m}}(\omega_{\mathrm{s}}) + \omega_{\mathrm{r0}}\boldsymbol{L}_{\mathrm{m}})\boldsymbol{x}_0^{\mathrm{d-q}} + \boldsymbol{B}_{\mathrm{m}}\boldsymbol{u}_{\mathrm{s0}}^{\mathrm{d-q}} = 0, \tag{24}$$

and afterwards, substituting obtained result into following equation:

$$\boldsymbol{i}_{\mathrm{s0}}^{\mathrm{d-q}} = \boldsymbol{C}_1\boldsymbol{x}_0^{\mathrm{d-q}}. \tag{25}$$

Values $\hat{\boldsymbol{x}}_0^{\mathrm{d-q}}$ and $\hat{\omega}_{\mathrm{r0}}$ can be calculated taking into consideration equations (14) and (15) and numerically solving a set of following non-linear equations:

$$\begin{cases}\left[\boldsymbol{A}(\omega_{\mathrm{s}}) + \hat{\omega}_{\mathrm{r0}}\boldsymbol{L} + (\boldsymbol{K}_1 + \hat{\omega}_{\mathrm{r0}}\boldsymbol{K}_2)\boldsymbol{C}_1\right]\hat{\boldsymbol{x}}_0^{\mathrm{d-q}} + \ldots \\ \quad\ldots + \boldsymbol{B}_1\boldsymbol{u}_{\mathrm{s0}}^{\mathrm{d-q}} + (\boldsymbol{B}_2(\omega_{\mathrm{s}}) - \hat{\omega}_{\mathrm{r0}}\boldsymbol{K}_2)\boldsymbol{i}_{\mathrm{s0}}^{\mathrm{d-q}} = 0. \\ \left[\left(\boldsymbol{i}_{\mathrm{s0}}^{\mathrm{d-q}}\right)^{\mathrm{T}} - \left(\hat{\boldsymbol{x}}_0^{\mathrm{d-q}}\right)^{\mathrm{T}}\boldsymbol{C}_1^{\mathrm{T}}\right]\boldsymbol{H}\hat{\boldsymbol{x}}_0^{\mathrm{d-q}} = 0\end{cases} \tag{26}$$

Using first equation from the set (26), vector $\hat{\boldsymbol{x}}_0^{\mathrm{d-q}}$ can be expressed as a function of $\hat{\omega}_{\mathrm{r0}}$. Therefore numerical solution of the set of equations (26) boils down to assuming of a search range of value $\hat{\omega}_{\mathrm{r0}}$ and finding a value, for which the second equation from the set (26) is met. It may be shown that on account of speed tuning signal ε properties, equations set (26) has one solution only.

Transfer function of the linearised MRAS-type estimator

Equations (16) – (18) can be used for obtaining matrix $\boldsymbol{K}(s)$ of transfer functions of the linearised MRAS-type estimator. This matrix makes it possible to describe the MRAS-type estimator with following linear equation:

$$\left[\Delta\hat{\omega}_{\mathrm{r}} \quad \Delta\hat{\boldsymbol{\psi}}_{\mathrm{r}}^{\mathrm{d-q}} \quad \Delta\hat{\boldsymbol{\psi}}_{\mathrm{s}}^{\mathrm{d-q}}\right]^{\mathrm{T}} = \boldsymbol{K}(s)\left[\Delta\boldsymbol{u}_{\mathrm{s}}^{\mathrm{d-q}} \quad \Delta\boldsymbol{i}_{\mathrm{s}}^{\mathrm{d-q}}\right]^{\mathrm{T}},$$

$$\boldsymbol{K}(s)=\begin{bmatrix} \boldsymbol{K}_{\omega u}^{(1\times2)}(s) & \boldsymbol{K}_{\omega i}^{(1\times2)}(s) \\ \boldsymbol{K}_{\psi_{\mathrm{r}}u}^{(2\times2)}(s) & \boldsymbol{K}_{\psi_{\mathrm{r}}i}^{(2\times2)}(s) \\ \boldsymbol{K}_{\psi_{\mathrm{s}}u}^{(2\times2)}(s) & \boldsymbol{K}_{\psi_{\mathrm{s}}i}^{(2\times2)}(s) \end{bmatrix}. \tag{27}$$

The sizes of matrix $\boldsymbol{K}(s)$ elements are given in element's superscripts in round brackets. Elements of the matrix $\boldsymbol{K}(s)$ are expressed as:

$$\begin{aligned}
\boldsymbol{K}_{\omega u}(s) &= \left[1 - K_{\mathrm{PI}}\boldsymbol{E}_{10}(\boldsymbol{S}_4 - \boldsymbol{F}_0)^{-1}\boldsymbol{E}_{40}\right]^{-1}\cdot\ldots \\
&\quad \ldots\cdot\left[K_{\mathrm{PI}}\boldsymbol{E}_{10}(\boldsymbol{S}_4 - \boldsymbol{F}_0)^{-1}\boldsymbol{B}_1\right], \\
\boldsymbol{K}_{\omega i}(s) &= \left[1 - K_{\mathrm{PI}}\boldsymbol{E}_{10}(\boldsymbol{S}_4 - \boldsymbol{F}_0)^{-1}\boldsymbol{E}_{40}\right]^{-1}\cdot\ldots \\
&\quad \ldots\cdot K_{\mathrm{PI}}\left[\boldsymbol{E}_{20} + \boldsymbol{E}_{10}(\boldsymbol{S}_4 - \boldsymbol{F}_0)^{-1}(\boldsymbol{E}_{30} + \boldsymbol{B}_3\boldsymbol{S}_2)\right], \\
\boldsymbol{K}_{\psi_{\mathrm{r}}u}(s) &= \boldsymbol{C}_2\boldsymbol{K}_{xu}(s), \quad \boldsymbol{K}_{\psi_{\mathrm{r}}i}(s) = \boldsymbol{C}_2\boldsymbol{K}_{xi}(s), \\
\boldsymbol{K}_{\psi_{\mathrm{s}}u}(s) &= \boldsymbol{C}_3\boldsymbol{K}_{xu}(s), \quad \boldsymbol{K}_{\psi_{\mathrm{s}}i}(s) = \boldsymbol{C}_3\boldsymbol{K}_{xi}(s), \\
\boldsymbol{K}_{xu}(s) &= \left[\boldsymbol{I}_4 - K_{\mathrm{PI}}(\boldsymbol{S}_4 - \boldsymbol{F}_0)^{-1}\boldsymbol{E}_{40}\boldsymbol{E}_{10}\right]^{-1}\cdot\ldots \\
&\quad \ldots\cdot(\boldsymbol{S}_4 - \boldsymbol{F}_0)^{-1}\boldsymbol{B}_1, \\
\boldsymbol{K}_{xi}(s) &= \left[\boldsymbol{I}_4 - K_{\mathrm{PI}}(\boldsymbol{S}_4 - \boldsymbol{F}_0)^{-1}\boldsymbol{E}_{40}\boldsymbol{E}_{10}\right]^{-1}\cdot\ldots \\
&\quad \ldots\cdot(\boldsymbol{S}_4 - \boldsymbol{F}_0)^{-1}(\boldsymbol{E}_{30} + \boldsymbol{B}_3\boldsymbol{S}_2 + K_{\mathrm{PI}}\boldsymbol{E}_{40}\boldsymbol{E}_{20}).
\end{aligned} \tag{28}$$

The correctness of the obtained matrix of transfer functions $\boldsymbol{K}(s)$ was verified in the Matlab-Simulink environment.

Results of the MRAS-type estimator stability analysis

The analysis of the MRAS-type estimator stability, for its different forms, was performed taking into consideration simultaneous random changes of R_{sm}, R_{rm}, $L_{\mathrm{s\sigma m}}$, $L_{\mathrm{r\sigma m}}$, L_{mm} parameters within assigned limits and with proper correlation of resistance changes. Investigation was performed for a large number of random parameters sets within assumed operating range of the induction motor. Operating range was defined with the range of stator winding supply frequency f_{s} and with the range of relative load $m_{\mathrm{m\%}}$, which was selected for each value f_{s}, so that the maximal load torque used in analysis was equal to the corresponding fraction of break-down torque, obtained for this frequency f_{s}. The stator winding supply voltage $\underline{u}_{\mathrm{s}}$ was calculated for each f_{s} value, according to the classical scalar control algorithm [11]. The result of investigation is the surface of instability occurrence probability P, obtained for assumed operating range. Moreover, the median surface of the relative error was obtained from the solution of equations (24) – (26), defined with dependence (22) for following quantities: ω_{r0}, $|\underline{\psi}_{\mathrm{s0}}|$, $|\underline{\psi}_{\mathrm{r0}}|$. Statistical analysis of the results was performed for each random set of parameters for each point of the assumed operating range. Investigations were performed for induction motor model rated at 3kW, using experimentally adjusted parameters K_{P} and T_{I} of the proportional-integral regulator. Exemplary plot of poles dispersion obtained for the changes of f_{s} and $m_{\mathrm{m\%}}$ for many random sets of parameters, for the form 3 of the MRAS-type estimator is shown in Fig. 4. Obtained surfaces of instability occurrence probability for different forms of the MRAS-type estimator are shown in Fig. 5. Obtained surfaces of the median $\delta\omega_{\mathrm{r0}}$, also for the different forms of MRAS-type estimator are shown in Fig. 6.

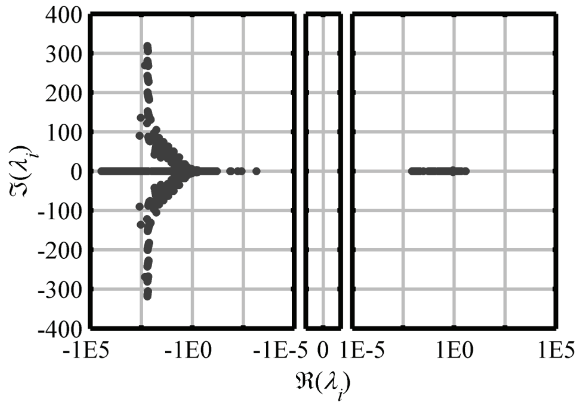

Fig. 4. Plot of the poles dispersion for the form 3 of the MRAS-type estimator (k=1,75)

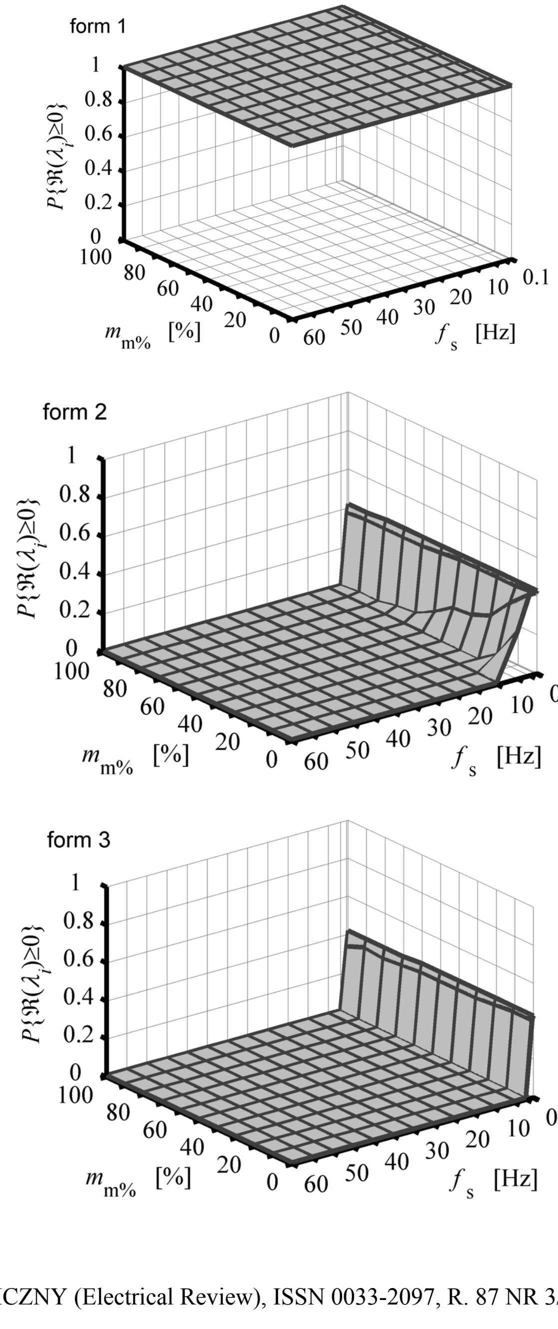

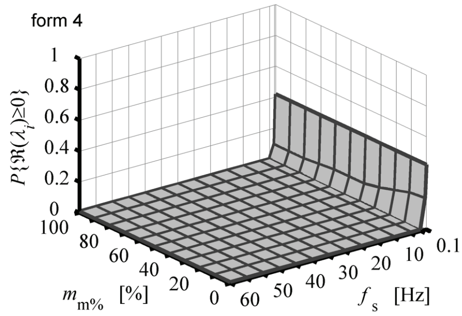

Fig. 5. Surfaces of instability occurrence probability for different forms of the MRAS-type estimator (for the form 3 parameter k=1,75)

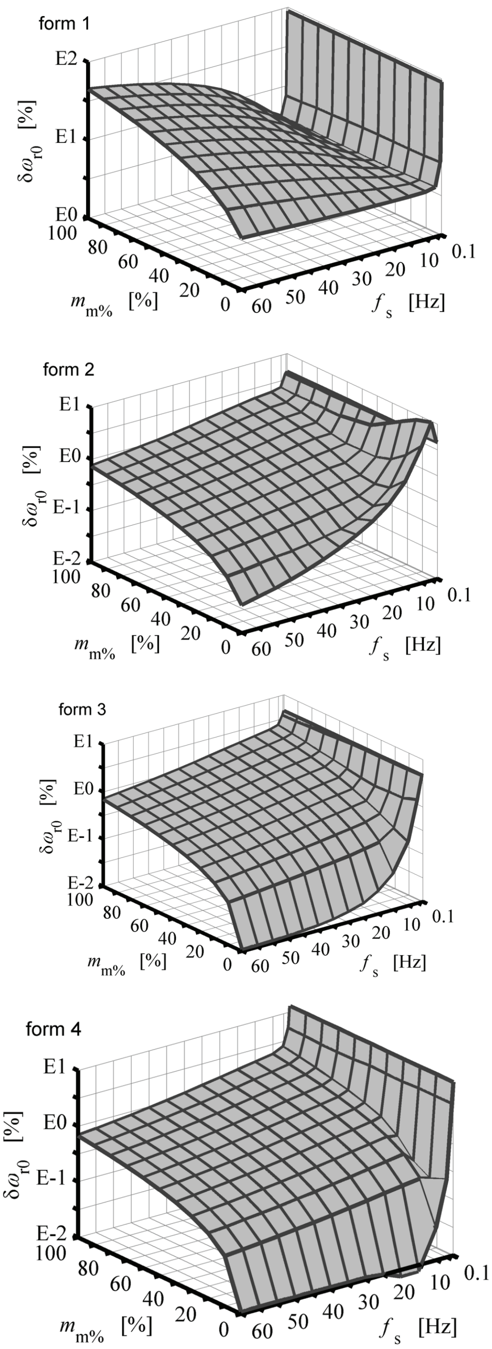

Fig. 6. Surfaces of the median of the speed reconstruction relative error for the different forms of the MRAS-type estimator (for the form 3 parameter k=1,75)

Conclusions

From the stability analysis performed for all forms of MRAS-type estimators, apart from parameter variations of the motor model, it is seen that considered estimators are stable within whole assumed operating range, except form 1 which has poles with real parts equal to zero (it is not asymptotically stable). However, after taking into consideration parameter variations of the motor model, it was found that instability is possible for the forms 2, 3, and 4, only for very small values of f_s. For the forms 3 and 4 instability occurrence probability is less. From the statistical analysis of steady-state reconstruction errors it is seen that the biggest immunity to deviations of motor model parameters is shown by form 3 of the MRAS-type estimator, while the results for forms 2, 3 and 4 are similar.

REFERENCES

[1] Ioannou P.A., Sun J., Robust Adaptive Control, Prentice Hall, 1996
[2] Vas P., Sensorless Vector And Direct Torque Control, Oxford University Press, 1998
[3] Orłowska-Kowalska T., Dybkowski M., Improved MRAS-type speed estimator for the sensorless induction motor drive, EPNC 2006, XIX Symposium, Maribor, Slovenia, June 28-30, 2006
[4] Niestrój R., Lewicki A., Białoń T., Pasko M., Odtwarzanie strumieni magnetycznych i prędkości obrotowej silnika indukcyjnego przy użyciu estymatora typu MRAS z obserwatorem Luenbergera w roli modelu adaptacyjnego, XLV SME 2009, Rzeszów – Krasiczyn 2009, 51-57
[5] Dybkowski M., Orłowska-Kowalska T., Analiza dynamiki prądowego estymatora MRAS strumienia i prędkości wirnika silnika indukcyjnego, *Przegląd Elektrotechniczny*, nr 6/2008, 165-168
[6] Sobczuk D. L., Application of ANN for control of PWM inverter fed induction motor drives, Ph.D. Thesis, Warsaw Uniwersity of Technology, 1999
[7] Żywiec A., Białoń T., Synteza obserwatora sprzężeń elektromagnetycznych silnika indukcyjnego przy wykorzystaniu algorytmów genetycznych, XXXIX SME 2003, Gdańsk – Jurata, CD
[8] Kubota H., Matsuse K., Nakano T., DSP-Based Speed Adaptive Flux Observer of Induction Motor, *IEEE Transactions of Industry Applications*, 29 (1993), No 2, 344-348
[9] Orłowska-Kowalska T., Bezczujnikowe układy napędowe z silnikami indukcyjnymi. Oficyna Wydawnicza Politechniki Wrocławskiej, Wrocław, 2003
[10] Kaczorek T., Teoria układów regulacji automatycznej, Wydawnictwa Naukowo-Techniczne, Warszawa 1977
[11] ACI3-1 System Document, C2000 Foundation Software, Texas Instruments Inc., December 2005

***Authors**: mgr inż. Roman Niestrój, Politechnika Śląska, Instytut Elektrotechniki i Informatyki, Zakład Maszyn Elektrycznych i Inżynierii Elektrycznej w Transporcie, ul. Akademicka 10a, 44-100 Gliwice, E-mail: roman.niestroj@polsl.pl; dr inż. Tadeusz Białoń, Politechnika Śląska, Instytut Elektrotechniki i Informatyki, Zakład Maszyn Elektrycznych i Inżynierii Elektrycznej w Transporcie, ul. Akademicka 10a, 44-100 Gliwice, E-mail: tadeusz.bialon@polsl.pl; prof. dr hab. inż. Marian Pasko, Politechnika Śląska, Instytut Elektrotechniki i Informatyki, Zakład Maszyn Elektrycznych i Inżynierii Elektrycznej w Transporcie, ul. Akademicka 10a, 44-100 Gliwice, E-mail: marian.pasko@polsl.pl;*